Influence of spin reorientation on magnetocaloric effect in $NdAl_2$: A microscopic model

P. J. von Ranke,[1,*] N. A. de Oliveira,[1] C. Mello,[1] D. C. Garcia,[1] V. A. de Souza,[1] and A. Magnus G. Carvalho[2]
[1]*Instituto de Física, Universidade do Estado do Rio de Janeiro—UERJ, Rua São Francisco Xavier, 524, 20550-013, Rio de Janeiro, Brazil*
[2]*Instituto de Física 'Gleb Wataghin,' Universidade Estadual de Campinas—UNICAMP, Caixa Postale. 6165, Campinas 13 083-970, São Paulo, Brazil*

(Received 23 May 2006; published 21 August 2006)

We report a theoretical investigation about the influence of the spin reorientation from easy magnetic direction ⟨001⟩ to the applied magnetic field direction ⟨111⟩ on the magnetocaloric properties of $NdAl_2$. This compound was fully investigated using a model Hamiltonian which includes the Zeeman-exchange interactions and the crystalline electrical field, which are responsible for the magnetic anisotropy. All theoretical results were obtained using the proper model parameters for $NdAl_2$, found in the literature. The existence of a minimum in magnetic entropy change below the phase transition was predicted and ascribed to the strong jump on the spin reorientation.

DOI: 10.1103/PhysRevB.74.054425 PACS number(s): 75.30.Sg, 75.10.Dg, 75.20.En

INTRODUCTION

In the last ten years much efforts have been dedicated to the development of new magnetocaloric materials due to the broad interest which runs from technologic applications, such as magnetic refrigeration that is based on the magnetocaloric effect, to the pure physical theoretical interest, such as several types and nature of phase transitions.[1] The magnetocaloric potential in given magnetic material is characterized by the two main thermodynamics quantities, namely ΔS_{mag} (the isothermal magnetic entropy change) and ΔT_{ad} (the adiabatic temperature change), which are observed upon changes in the external magnetic field. The experimental discovery of giant magnetocaloric effect around room temperature in some magnetic materials such as $Gd_5(Si_xGe_{1-x})_4$,[2] $MnFeP_{0.45}As_{0.55}$,[3] $MnAs_{1-x}Sb_x$,[4,5] and $La(Fe_{1-x}Si_x)_{13}$,[6,7] and its hydrides enhanced the interest in magnetocaloric effect due to the potential applications of these materials to work as refrigerant materials in magnetic refrigeration at room temperature. The potential application of a near-room temperature magnetic refrigerator was firstly reported by G. V. Brown.[8] The first theoretical descriptions, using a phenomenological model and in which the magnetic state equations were solved self-consistently and applied to the giant magnetocaloric materials $Gd_5(Si_xGe_{1-x})_4$, $MnFeP_{0.45}As_{0.55}$, and $MnAs_{1-x}Sb_x$, were reported by some of us (Refs. 9–11). The signature of giant magnetocaloric materials is the abrupt change in the order parameter, magnetization, at Curie temperature (first-order magnetic phase transition), which is coupled to crystallographic phase transition or a high change in lattices parameters. More recently the experimental and theoretical investigations led to the discovery of the colossal magnetocaloric effect where the lattice entropy plays fundamental role in order-disorder magnetic process due to the magnetoelastic interaction.[12–14]

Another important aspects of magnetocaloric materials is concerned with the magnetic anisotropy effects which leads, for example, to different behaviors for temperature and magnetic field dependence of the magnetization for different choices of applied magnetic field direction in crystallographic referential frame. Since the magnetocaloric potential quantities, ΔS_{mag} and ΔT_{ad}, depend on the magnetization response to the applied magnetic field change, the choice of the applied magnetic field direction in the crystal, in an anisotropic magnetic material, leads to different values for ΔS_{mag} and ΔT_{ad}. We are interested in the anisotropy caused, in rare earth intermetallic compounds due to the crystalline electrical field (CEF) interaction. In rare-earth the CEF interaction, in general, destroys the magnetic symmetry due to the total or partial break of $(2J+1)$-times degenerated $4f$ Hund's ground states. As a consequence, some interesting physical effects can appear—for example, the pure paramagnetic $PrNi_5$ compound cools down when submitted to external magnetic field in an adiabatic process below 14 K for magnetic field change from 0 to 5 T (the so-called anomalous MCE). Therefore, as far as we know, $PrNi_5$ is the only paramagnetic system that has its magnetic entropy increased with the magnetic field, and this anomaly could be quantitatively explained by the CEF anisotropy effects.[15,16] Recently, experimental measurements of ferromagnetic single-crystal $DyAl_2$ showed anomalous magnetocaloric effect when the external magnetic field change is considered along the ⟨111⟩ crystallographic direction,[17] confirming the previous theoretical prediction[18] based on the study of CEF anisotropy of this material.

In this paper, we present the theoretical results of a full investigation on the magnetic and magnetocaloric properties of $NdAl_2$ considering the magnetic field change along the three main crystallographic directions, namely ⟨001⟩ (the easy magnetic direction), ⟨101⟩, and ⟨111⟩. We started with the microscopic model where the interactions included in the magnetic model Hamiltonian are (i) the Zeeman interaction, (ii) the exchange interaction in the molecular field approximation, and (iii) the cubic CEF anisotropic interaction. The lattice entropy was treated in the Debye assumptions. From the Hamiltonian, the magnetic state equation is obtained and the temperature and field dependence of magnetization are calculated, self-consistently, in the three main directions. When the magnetic field is applied in the ⟨111⟩ direction, a predicted critical temperature $T_R \sim 50$ K, is calculated at

magnetic field $H \sim 3.2$ T, where the magnetization jump (spin reorientation process) along $\langle 111 \rangle$ occurs. The influence of this reorientation on the magnetocaloric potential ΔS_{mag} and ΔT_{ad} was investigated.

THEORY

The intermetallic $NdAl_2$ compound presents cubic crystallographic symmetry and the magnetism comes from the localized magnetic moment due to the unfilled $4f$ states in Nd ions. The magnetic anisotropy in this compound comes from the CEF interaction which is described by two parameters in the CEF Hamiltonian since Nd in $NdAl_2$ is surrounded by atomic charges with cubic symmetry. The total Hamiltonian to describe the magnetism of $NdAl_2$ is the sum of CEF and magnetic Hamiltonians, the last one containing the exchange interaction (in molecular field approximation) and the Zeeman interaction and is given by:

$$\hat{H} = \hat{H}_{CEF} + \hat{H}_{MAG}, \tag{1}$$

where

$$\hat{H}_{CEF} = W\left[\frac{X}{F_4}(O_4^0 + 5O_4^4) + \frac{(1-|X|)}{F_6}(O_6^0 - 21O_6^4)\right], \tag{2}$$

and

$$\hat{H}_{MAG} = -g\mu_B[(H\cos\alpha + \lambda M_x)J_x + (H\cos\beta + \lambda M_y)J_y + (H\cos\gamma + \lambda M_z)J_z]. \tag{3}$$

Relation (2) is the single-ion CEF Hamiltonian written in the Lea, Leask, and Wolf (LLW) representation[19] where W gives the CEF energy scale and X, $(-1 < X < 1)$ gives the relative contributions of the fourth and the sixth degree in O_n^m Stevens' equivalent operators.[20] The dimensionless constants F_4 and F_6 (for Nd, in cubic crystalline symmetry) have the values $F_4 = 60$ and $F_6 = 2520$, tabulated in Ref. 19.

Relation (3) is the single-ion magnetic Hamiltonian, taken in the molecular field approximation, where g is the Lande factor, μ_B is the Bohr magneton, and H is the intensity of the external magnetic field applied on an arbitrary direction forming the angles α, β, and γ with the cubic crystallographic axis x, y, and z, respectively (z is the considered quantization direction). The three components of the magnetization and the total angular momentum vectors are M_k and $J_k (k = x, y, z)$, respectively. The intensity of the magnetization, M, and the component of the magnetization vector, M_h, along the applied magnetic field direction are:

$$M = \sqrt{M_x^2 + M_y^2 + M_z^2}, \tag{4}$$

$$M_h = \cos(\alpha) \,.\, M_x + \cos(\beta) \,.\, M_y + \cos(\gamma) \,.\, M_z. \tag{5}$$

The components of the magnetization vector are obtained by the mean thermodynamic values of the magnetic moments:

$$M_k = g\mu_B \frac{\sum_j \langle E_j | J_k | E_j \rangle \exp(E_j k_B T)}{\sum_j \exp(E_j k_B T)}, \tag{6}$$

where E_j and $|E_j\rangle$ are the energy eigenvalues and eigenvectors of the Hamiltonian (1). It should be observed that E_j and $|E_j\rangle$ depend on the three magnetization vector components. Therefore, in order to obtain the magnetization components from relation (6) it is necessary to solve a *three-dimensional* self-consistent problem numerically.

The total entropy S necessary to calculate the magnetocaloric potential in $NdAl_2$ has three main contributions and is given by

$$S(H,T) = S_{mag}(H,T) + S_{lat}(T) + S_{el}(T). \tag{7}$$

The magnetic entropy S_{mag} can be determined by the general relation:

$$S_{mag}(T,H) = \left(\frac{1}{T}\right)\frac{\sum_j E_j \exp(-E_j/k_B T)}{\sum_j \exp(-E_j/k_B T)} + k_B \ln\left[\sum_j \exp\left(-\frac{E_j}{k_B T}\right)\right]. \tag{8}$$

The temperature and magnetic field dependence of the above magnetic entropy is not trivial, since for a given pair (T,H), the $M_k = M_k(T,H,M_l)$, must be determined self-consistently in order to obtain the proper set of the energy eigenvalues, E_j, from the total Hamiltonian, relation (1), to update relation (8).

The lattice entropy can be calculated using the Debye relation:

$$S_{lat} = -3R\ln\left[1 - \exp\left(-\frac{\Theta_D}{T}\right)\right] + 12R\left(\frac{T}{\Theta_D}\right)^3 \int_0^{\Theta_D/T} \frac{x^3 dx}{\exp(x) - 1}, \tag{9}$$

where R is the gas constant and Θ_D is the Debye temperature.

The electronic entropy can be obtained from the standard relation

$$S_{el} = \bar{\gamma} T, \tag{10}$$

where $\bar{\gamma}$ is the electronic heat capacity coefficient.

The magnetocaloric potential, i.e., the isothermal entropy change, $-\Delta S$, and the adiabatic temperature change, ΔT_{ad}, that occur for changes in the external magnetic field are obtained from relation (7), plotting the total entropy vs temperature with and without external magnetic field and computing the isothermal and adiabatic differences in these two pairs of curves,

$$-\Delta S(T,H) = S(T,H=0) - S(T,H), \tag{11}$$

$$\Delta T_{ad}(T,H) = T(T,H \neq 0) - T(T,H=0). \tag{12}$$

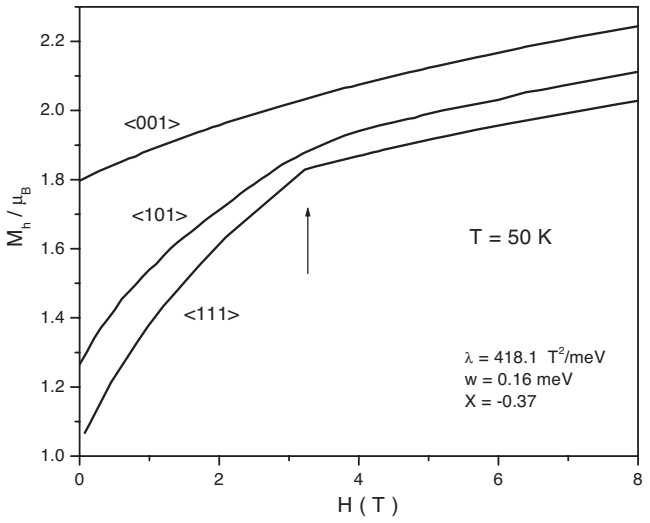

FIG. 1. Magnetic field dependence of the magnetization components along the applied magnetic field in three crystallographic direction ⟨001⟩ easy magnetic direction, ⟨101⟩ and ⟨111⟩ for $NdAl_2$ compound, calculated at $T=50$ K.

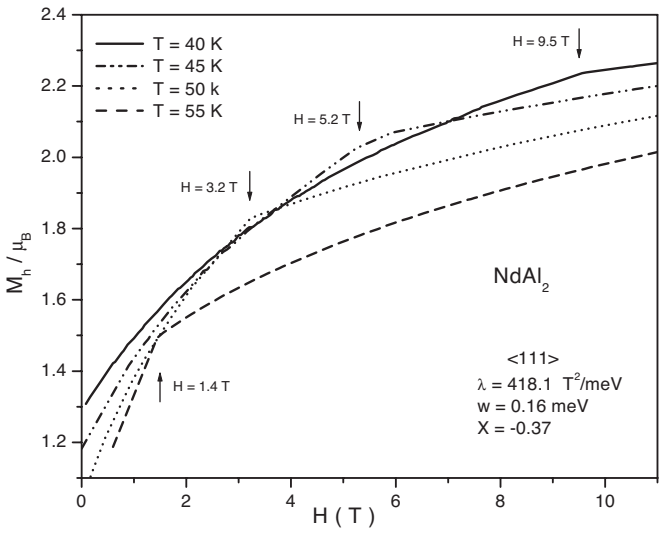

FIG. 2. Magnetic field dependence of the magnetization components along the applied field in ⟨111⟩, for $NdAl_2$ compound, calculated for different temperatures $T=40$ K (solid curve), $T=45$ K (dashed-dotted-dotted curve), $T=50$ K (dotted curve) and $T=55$ K (dashed curve). The arrows indicate the critical field where the spin reorientation occurs.

APPLICATION TO $NdAl_2$ AND DISCUSSION

The model parameters necessary to apply the above model to investigate the magnetic anisotropy in $NdAl_2$ are $W=0.16$ meV, $X=-0.37$, and $\lambda=418.1$ T^2/meV, which were obtained from Ref. 21. We have considered the cubic crystalline axes of $NdAl_2$ oriented in the Cartesian axes in such a way that the quantization axis was considered in $z\langle 001\rangle$, the easy $NdAl_2$ magnetic direction. Figure 1 shows the components of magnetization, M_h, vs magnetic field considered in the three main crystallographic directions ⟨001⟩, ⟨101⟩, and ⟨111⟩, calculated at $T=50$ K. Its worth noticing that the components are obtained from relation (5) considering the proper cosines which orient the applied magnetic field H, namely: $\cos\alpha=0$, $\cos\beta=0$, and $\cos\gamma=1$ for the ⟨001⟩ direction; $\cos\alpha=1/\sqrt{2}$, $\cos\beta=0$, and $\cos\gamma=1/\sqrt{2}$ for the ⟨101⟩ direction; and $\cos\alpha=1/\sqrt{3}$, $\cos\beta=1/\sqrt{3}$, and $\cos\gamma=1/\sqrt{3}$ for the ⟨111⟩ direction. The choice of our orientation axes is the usual one and differs from the previous choice of axes adopted by P. Bak.[22] In our referential system, the numerical solution, for the three magnetization components M_x, M_y, and M_z, must be obtained entering with initial (try magnetization components) in magnetic Hamiltonian, relation (3), and solving a three-dimensional self-consistent problem, computing simultaneously the final (solution magnetization components) obtained from relation (6). From Fig. 1 we can note that the easy magnetic orientation occurs for magnetic field applied in ⟨001⟩ direction and the hard direction occurs for ⟨111⟩. The kink, indicated by the arrow in Fig. 1, that appears in the curve of M_h vs H, in the ⟨111⟩ direction, occurs at the critical magnetic field of about $H_R=3.2$ T and is due to the reorientation spin process, i.e., for $H>H_R$, the magnetization vector is oriented in the magnetic field direction. An accurate analysis shows that the critical spin reorientation field depends on the temperature. Figure 2 shows some isothermic curves for M_h vs H (H applied in the ⟨111⟩ direction) and the arrows indicate the different values of the H_R which change with the temperature. It is worth noticing that for temperatures greater than $T=57$ K and lower than $T=38$ K, the kink could not be any more observed in M_h vs H curves.

Figure 3 shows the $NdAl_2$ temperature dependence of magnetization M_h calculated at zero field and at fields equals to $H=1.4$ T and $H=3.2$ T, applied along the ⟨111⟩ direction. The calculated Curie temperature (in zero field) is $T_c=64$ K, which is in good agreement with the reported experimental value[21,23] for $NdAl_2$. The curves of M_h vs T calculated for

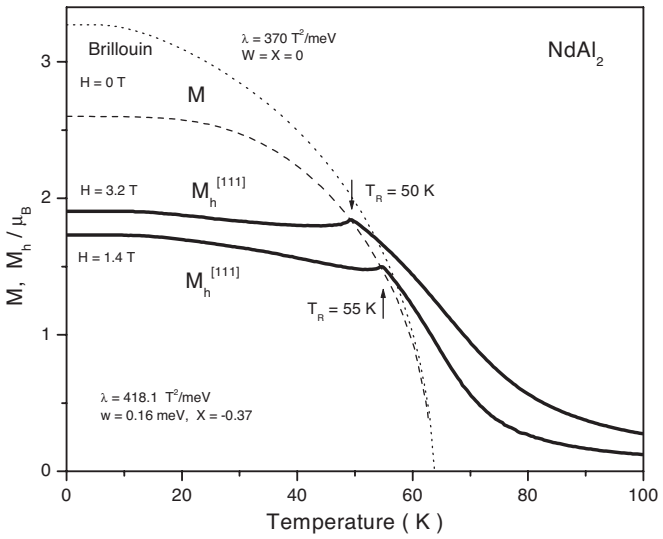

FIG. 3. The temperature dependence of magnetization in $NdAl_2$ for $H=0$, $H=1.4$ T, and $H=3.2$ T applied in the ⟨111⟩ direction. The arrows indicate the critical temperatures where the spin orientation occurs. The dotted curve represents the Brillouin magnetization curve.

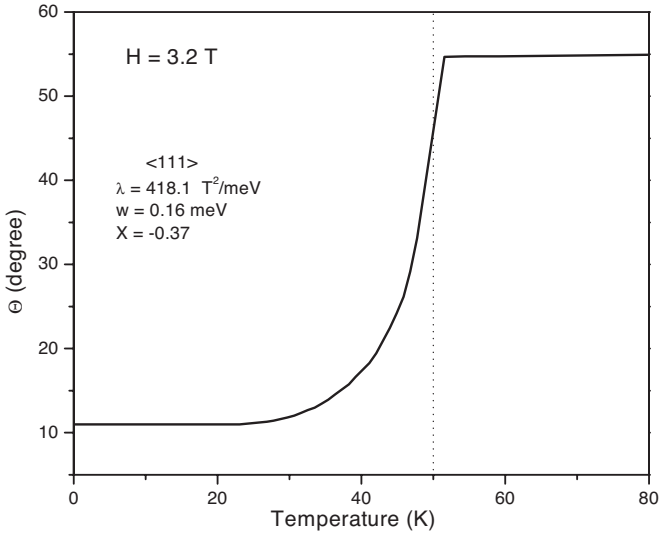

FIG. 4. The temperature dependence of the polar angle formed between the easy magnetic direction ⟨001⟩ and the magnetization vector direction, calculated at $H=3.2$ T. The dotted line indicates the spin reorientation temperature.

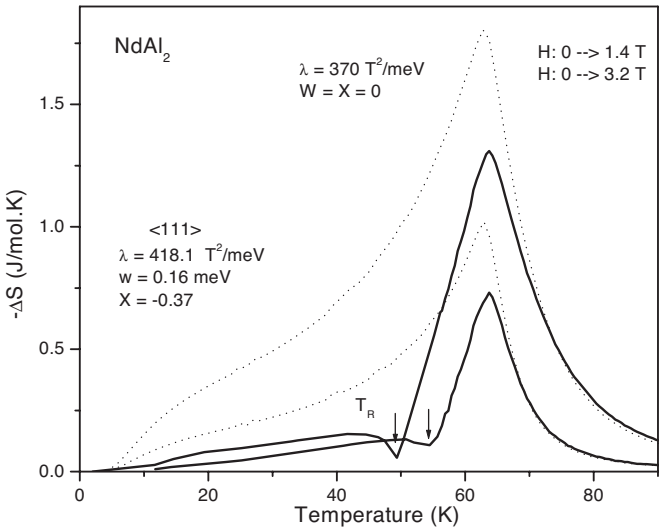

FIG. 5. The temperature dependence of ΔS for $NdAl_2$ for a magnetic field changes from 0 to 1.4 T and from 0 to 3.2 T, in the ⟨111⟩ direction. The dotted curves shows the ΔS vs T for the same magnetic field changes without CEF interaction ($W=0$ meV). The temperatures where the spin reorientation occurs are indicated by arrows.

magnetic fields $H=1.4$ T and $H=3.2$ T present a small peak at critical temperatures $T_R=55$ K and 50 K, respectively. We address the origin of these theoretical predicted peaks to a critical reorientation spin temperature. Note that we have chosen the values of $H=1.4$ T and $H=3.2$ T to calculate M_h vs T, shown in Fig. 3, since we have previously determined, in Fig. 2, these values as the critical fields for the spin reorientation in the isothermic curves with $T=55$ K and 50 K.

Another interesting behavior, due to the anisotropy, is the strong CEF-quenching effect in the magnetic moment of Nd in $NdAl_2$ compound. The dashed curve in Fig. 3 is the magnetization, M, calculated at zero field which presents a saturation values of $M_S \sim 2.6\ \mu_B$ (less than the Nd-free ion value $M_S \sim 3.27\ \mu_B$). The dotted curve in Fig. 3 is the magnetization without CEF interaction ($W=0$), i.e., the Brillouin curve for Nd in which the exchange parameter was adjusted ($\lambda=370\ T^2/meV$) to reproduces the Curie temperature of $NdAl_2$. Therefore, the reduction of the magnetic moment due to CEF interaction is about 20%, and its influence on the magnetocaloric effect will be discussed below.

Figure 4 shows the temperature dependence of the polar angle, $\Theta(T,H)$, between the z easy magnetic direction axis and the magnetization vector calculated for a magnetic field of $H=3.2$ T. The temperature and magnetic field dependence of $\Theta(T,H)$ is obtained under self-consistent solution of the three components of magnetization vector and using the following relation:

$$\tan \Theta(T,H) = \frac{\sqrt{M_x^2(T,H) + M_y^2(T,H)}}{M_z(T,H)}. \qquad (13)$$

The increase in $\Theta(T,H)$ with the temperature is not linear. For $T=0$ K the applied magnetic field of $H=3.2$ T produces an angular displacement of about $\Theta \sim 11$ degree which stays almost constant until the $T \sim 40$ K where the spin reorientation starts and at about $T \sim 50$ K the magnetization vector is aligned in the ⟨111⟩ magnetic field direction, i.e., $\Theta=\tan^{-1}(\sqrt{2})$. The spin alignment occurs continuously in a broad temperature windows of about 10 K, characterizing a second-order phase transition process.

Figure 5 shows the temperature dependence of $-\Delta S$ for magnetic field changes from 0 to 1.4 T and from 0 to 3.2 T in $NdAl_2$ (solid curves). The dotted curves in Fig. 5 were obtained in the absence of CEF interaction ($W=0$). The higher peaks at Curie temperature and large area under the $-\Delta S$ vs T when the CEF interaction is removed (compared to the results with the presence of CEF interaction in $NdAl_2$) are associated with the strong quenching effect on the magnetic moment discussed above and showed in Fig. 3. Besides the quenching, the CEF leads to an anomalous decrease which occurs in both $-\Delta S$ vs T curves near Curie temperature (see the arrows indicating the minima, in Fig. 5). This anomalous behavior is due to the spin reorientation process since this calculation was performed considering the magnetic field applied in ⟨111⟩ direction where the jump in magnetization direction exist as showed in Fig. 4. This anomalous MCE-effect does not exist if we calculate the $-\Delta S$ vs T curve, considering the magnetic field change in the easy magnetic direction, ⟨001⟩, not shown in this work. It is worth noticing that a similar behavior was experimentally observed by A. L. Lima and co-workers[17] in the $DyAl_2$ single crystal, in which the magnetic field was applied in a noneasy magnetic direction.

In the first view, the small peaks observed in M_h vs T could lead to a wrong interpretation in which these peaks increase the magnetic order (around the T_R) and, consequently, decrease the magnetic entropy around T_R, leading to an increase in the $-\Delta S$ around T_R. In order to explain this point, we have plotted in the same graphic of Fig. 6 the M_h [the magnetization component along the magnetic field, re-

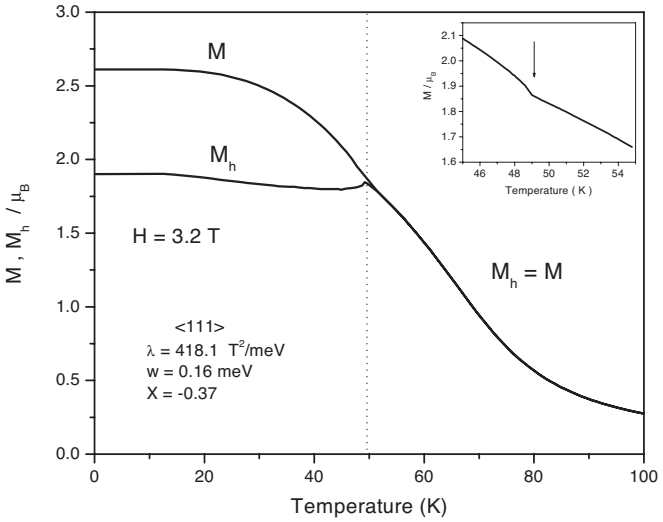

FIG. 6. The temperature dependence of magnetization M and the component, M_h, in $NdAl_2$ for $H=3.2$ T applied in the $\langle 111\rangle$ direction. The inset shows the detail of M vs T, and the arrow indicate the decreasing in M at the reorientation spin temperature.

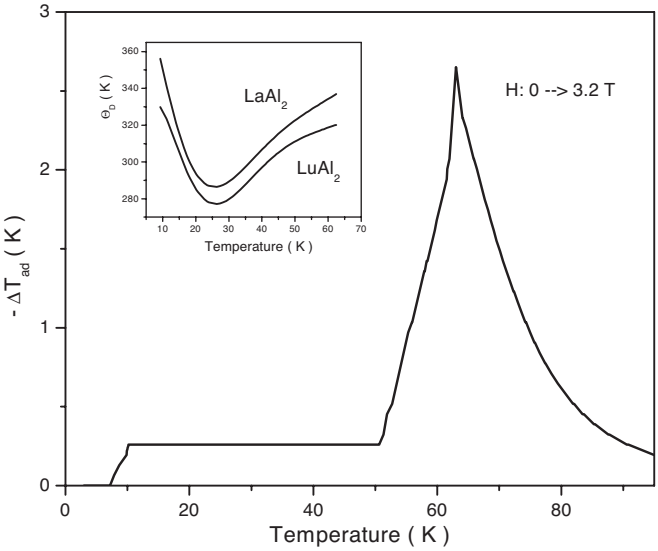

FIG. 7. The temperature dependence of ΔT_{ad} for $NdAl_2$ for a magnetic field change from 0 to 3.2 T, in the $\langle 111\rangle$ direction. The inset shows the temperature dependence of the Debye temperature obtained from $LaAl_2$ and $LuAl_2$ and used in the calculation of the $NdAl_2$ lattice entropy.

lation (5)] and M [the magnetization intensity, relation (4)] vs temperature for magnetic field intensity of $H=3.2$ T in the $\langle 111\rangle$ direction. As expected, $M>M_h$ for $T<T_R=50$ K and $M=M_h$ for $T>T_R$ since after the spin reorientation both magnetization vector and the applied magnetic field have the same direction. Contrary to M_h, the intensity of magnetization, M, presents a small decrease around T_R as shown in the inset of Fig. 6. Therefore, the increase in magnetic entropy, and consequently a decreasing in $-\Delta S$ around T_R, should be observed in accordance with our calculation. It is worth noticing that a pure quantum-mechanical effect is responsible for the decreasing in the magnetization intensity since it occurs due to the quenching of the total orbital moment of the $4f$ shell (the CEF-quenching effects depend on the spin orientation in the crystallographic axes). A semiclassical magnetic model, in which the magnetization vector is considered with constant intensity, does not predicts the anomalous decreasing in $-\Delta S$ shown in Fig. 5.

In order to calculate the adiabatic temperature change ΔT_{ad} defined in relation (12), we must include the electronic entropy, relation (10), in which the electronic coefficient $\bar{\gamma}=4.90$ J/mol K^2 was used, and the lattice entropy given by relation (9). In general, in RAl_2 (R=rare earth) compounds, the electronic entropy contribution for ΔT_{ad} calculation can be neglected compared to the lattice ones. In spite of obtaining an accurate lattice contribution to the total entropy in $NdAl_2$, we used the temperature dependence of the Debye temperature for non-magnetic compounds $LaAl_2$ and $LuAl_2$ obtained from heat capacity experimental data.[24,25] The inset in Fig. 7 shows the graphics of Θ_D vs T for $LaAl_2$ and $LuAl_2$ which have a considerable variation in the temperature range of ordered ferromagnetic phase of $NdAl_2$. Above $T=100$ K, the Debye temperature of $LaAl_2$ and $LuAl_2$ are almost constant, not shown in this work.

The lattice entropy was determined assuming that heat capacity varies linearly in the RAl_2 series of intermetallic compounds when the R component changes across the series from non-magnetic La to nonmagnetic Lu. On these assumptions, the expression for the lattice entropy can be determined by the following average expression:

$$S_{latt}^{R}(T)=\frac{(14-n)S_{latt}^{\mathrm{La}}(T)+nS_{latt}^{\mathrm{Lu}}(T)}{14}, \qquad (14)$$

where n gives the relative position of the rare earth element in rare earth series, in our case, for Nd systems, we have $n=3$.

Figure 7 shows the calculated ΔT_{ad} vs T for magnetic field change from 0 to 3.2 T applied in the $\langle 111\rangle$ direction. Instead of a decreasing of ΔT_{ad} below the Curie temperature (as occurs in $-\Delta S$). a tablelike magnetocaloric effect behavior emerges in the interval temperature from 10 to 50 K associated with the nonconstant Debye temperature. Above $T=50$ K, the spin reorientation phase transition has been completed and a normal profile for the magnetocaloric curve is observed.

FINAL COMMENTS

Using a microscopic model Hamiltonian that includes the anisotropy due to the CEF effect, we have quantitatively investigated, and discussed the magnetic and magnetocaloric properties in $NdAl_2$ considering an extension of the two-dimensional mean field theory devised by P. Bak. The focus was concentrated on the spin reorientation phase transition process and its influence on the magnetocaloric thermodynamic quantities. The peaks in the temperature dependence of magnetization component, along the $\langle 111\rangle$ direction, were predicted and associated with the spin reorientation process. We stress here that similar peak was recently reported,[17] experimentally, in a single crystal of $DyAl_2$. Another similar magnetic compound that deserves to be investigated is

$HoAl_2$, since its spin reorientation occurs from ⟨110⟩ easy magnetic direction to the ⟨100⟩ direction, at about $T_R=21$ K, under first-order transition process[26,27] (which occurs in a very narrow temperature range $T_R=20.9\pm0.6$ K and presents a hysteresis of about 2 K).

The theoretical anomalous minimum in the $-\Delta S$ curve, below the Curie temperature, was predicted in $NdAl_2$, and the origin was fully investigated and ascribed to the quenching effect that occurs in the intensity of the magnetization vector associated with the CEF anisotropy. However, our theoretical prediction requires experimental investigation on a $NdAl_2$ single crystal, in order to be confirmed. The studies of the CEF anisotropy influence in magnetocaloric materials[17] have been just starting and may have a great impact on experimental investigations in order to design new magnetocaloric materials to be used as a refrigerant in magnetic refrigerators.

ACKNOWLEDGMENTS

We acknowledge financial support from CNPq—Conselho Nacional de Desenvolvimento Científico e Tecnológico—Brazil, CAPES and FAPERJ—Fundação de Amparo à Pesquisa do Estado do Rio de Janeiro. This work was also partially supported by PRONEX No. E-26/ 171.168/2003 from FAPERJ/CNPq.

*Corresponding author. Email address: vonranke@nitnet.com.br

[1] A. M. Tishin and Y. I. Spichkin, *The Magnetocaloric Effect and Its Applications* (Institute of Physics, Bristol, 2003).
[2] V. K. Pecharsky and K. A. Gschneidner, Jr., Phys. Rev. Lett. **78**, 4494 (1997).
[3] O. Tegus, E. Brück, K. H. J. Buschow, and F. R. de Boer, Nature **415**, 150 (2002).
[4] H. Wada and Y. Tanabe, Appl. Phys. Lett. **79**, 3302 (2001).
[5] H. Wada, T. Morikawa, K. Taniguchi, T. Shibata, Y. Yamada, and Y. Akishige, Physica B **328**, 114 (2003).
[6] F. Hu, B. Shen, J. Sun, Z. Cheng, G. Rao, and X. Zhang, Appl. Phys. Lett. **78**, 3675 (2001).
[7] A. Fujita, S. Fujieda, Y. Hasegawa, and K. Fukamichi, Phys. Rev. B **67**, 104416 (2003).
[8] G. V. Brown, J. Appl. Phys. **47**, 3673 (1976).
[9] P. J. von Ranke, N. A. de Oliveira, and S. Gama, J. Magn. Magn. Mater. **277**, 78 (2004).
[10] P. J. von Ranke, N. A. de Oliveira, and S. Gama, Phys. Lett. A **320**, 302 (2004).
[11] P. J. von Ranke, A. de Campos, L. Caron, A. A. Coelho, S. Gama, and N. A. de Oliveira, Phys. Rev. B **70**, 094410 (2004).
[12] S. Gama, Adelino A. Coelho, Ariana de Campos, A. M. Carvalho, F. C. G. Gandra, P. von Ranke, and N. A. de Oliveira, Phys. Rev. Lett. **93**, 237202 (2004).
[13] P. J. von Ranke, N. A. de Oliveira, C. Mello, A. M. Carvalho, and S. Gama, Phys. Rev. B **71**, 054410 (2005).
[14] P. J. von Ranke, S. Gama, A. A. Coelho, A. de Campos, A. M. Carvalho, F. C. G. Gandra, and N. A. de Oliveira, Phys. Rev. B **73**, 014415 (2006).
[15] P. J. von Ranke, V. K. Pecharsky, K. A. Gschneidner, and B. J. Korte, Phys. Rev. B **58**, 14436 (1998).
[16] P. J. von Ranke, M. A. Mota, D. F. Grangeia, A. M. Carvalho, F. C. G. Gandra, A. A. Coelho, A. Caldas, N. A. de Oliveira, and S. Gama, Phys. Rev. B **70**, 134428 (2004).
[17] A. L. Lima, A. O. Tsokol, K. A. Gschneidner, Jr., V. K. Pecharsky, T. A. Lograsso, and D. L. Schlagel, Phys. Rev. B **72**, 024403 (2005).
[18] P. J. von Ranke, I. G. de Oliveira, A. P. Guimaraes, and X. A. da Silva, Phys. Rev. B **61**, 447 (2000).
[19] K. R. Lea, M. J. M. Leask, and W. P. Wolf, J. Phys. Chem. Solids **33**, 1381 (1962).
[20] K. W. H. Stevens, Proc. Phys. Soc., London, Sect. A **65**, 209 (1952).
[21] H. G. Purwins and A. Leson, Adv. Phys. **39**, 309 (1990).
[22] P. Bak, J. Phys. C **7**, 4097 (1974).
[23] N. Nereson, C. Olsen, and G. Arnold, J. Appl. Phys. **37**, 4575 (1996).
[24] C. Deenadas, A. W. Thompson, R. S. Graig, and W. E. Wallace, J. Phys. Chem. Solids **32**, 1843 (1971).
[25] T. Inoue, S. G. Sankar, R. S. Graig, W. E. Wallace, and K. A. Gschneidner, Jr., J. Phys. Chem. Solids **38**, 487 (1997).
[26] B. Barbara, J. X. Boucherle, B. Michelutti, and M. F. Rossignol, Solid State Commun. **31**, 477 (1979).
[27] B. Barbara, M. F. Rossignol, and J. X. Boucherle, Phys. Lett. **55A**, 321 (1975).